Kinetics of advanced oxidative leaching of pyrite in a potassium peroxydisulphate solution

J. Ma[1], Y. Tang[1], D.Q. Yang[1], and P. Pei[1]

Affiliation:
[1]Mining College, Guizhou University, Guiyang, China

Correspondence to:
Y. Tang

Email:
caseyty@163.com

Dates:
Received: 9 Apr. 2019
Revised: 1 Jul. 2019
Accepted: 28 Nov. 2019
Published: February 2020

How to cite:
Ma, J., Tang, Y., Yang, D.Q., and Pei, P.
Kinetics of advanced oxidative leaching of pyrite in a potassium peroxydisulphate solution.
The Southern African Insitute of Mining and Metallurgy

DOI ID:
http://dx.doi.org/10.17159/2411-9717/710/2020

ORCiD ID:
J. Ma
https://orchid.org/0000-0003-0999-5940

Synopsis

This study investigates the leaching kinetics of gold-bearing pyrite in the potassium peroxydisulphate system and the potassium peroxydisulphate-ferrous sulphate combined system, using potassium peroxydisulphate as an oxidizing agent. Experimental results indicate that the pyrite leaching rate is roughly proportional to the potassium sulphate concentration. The pyrite leaching rate also increases with temperature, and is 48.19% faster at 70°C than at 30°C. Additionally, the pyrite leaching rate is inversely proportional to the particle size; the leaching rate of < 0.038 mm particles is 44.31% greater than that of 0.180–0.120 mm particles. At 70°C, the concentration of ferrous sulphate has no effect. However, at the more typical leaching temperature of 30°C, the addition of ferrous sulphate and hydrogen peroxide can increase the rate of leaching. Therefore, the kinetics of pyrite leaching in the potassium peroxydisulphate system at 70°C and in the potassium peroxydisulphate-ferrous sulphate combined system at normal temperatures were investigated in detail. Pyrite leaching kinetics follows the formula $kt = 1 - 2/3x - (1 - x)^{2/3}$ where solid film diffusion is the limiting process. The effective activation energy of pyrite leaching in the temperature range 30–70°C was 65.30 kJ/mol. Pyrite had a regular crystal habit prior to leaching, but exhibited faviform holes after leaching. These results provide a basis for effective leaching of gold from gold-bearing pyrite ores using the advanced oxidative leaching system.

Keywords
gold-bearing pyrite, high-grade oxidation, leaching dynamics, activation energy.

Introduction

Pyrite is one of the most common sulphide ores, and is an important carrier of gold, silver, and platinum (Gu *et al.*, 2010). In concert with China's rapid economic progress, the demand for gold continues to increase every year, such that difficult-to-process micro-disseminated gold deposits constitute a major category of gold resources. Gold contained in micro-disseminated gold deposits is typically encased in pyrite, such that the gold is physically shielded and thereby difficult to react with the leaching agent. This condition leads to relatively low leaching rates, typically less than 80%. Therefore, pretreatment is necessary prior to leaching of a micro-disseminated gold ore. Common pretreatment methods include oxidizing roast, microbial oxidation, and chemical hydrometallurgical oxidation (Hu *et al.*, 2017). The method of chemical hydrometallurgical oxidation has recently gained attention because of its advantages, including less pollution and a shorter treatment period (Gozmen *et al.*, 2009).

Chemical hydrometallurgical oxidation utilizes strong oxidants in solution to destroy the pyrite structure and expose the contained gold to subsequent chemical processes. The mostly frequently reported chemical hydrometallurgical oxidation systems for pyrite include $Fe_2(SO_4)_3$, HNO_3, H_2SO_4, and $HClO_4$ (Zhao *et al.*, 2016). The high-grade oxidation method, which has been used in wastewater treatment, has yet to be widely used in mineral processing (Hillesa *et al.*, 2016). However, experimental pretreatments performed on micro-disseminated gold ores have yielded promising results, with leaching rates of up to 86.09% (Tang *et al.*, 2015). Peroxysulphate oxidizes pyrite by generating sulphate radical anions. To better understand the leaching characteristics and kinetics of high-grade oxidation of pyrite based on sulphate radical anion oxidation, controlled experiments were performed in the $K_2S_2O_8$-$FeSO_4$ system. The leaching kinetics were investigated based on the experimental results, and SEM analyses were performed on the oxidation products. This study provides theoretical support and practical guidance for the high-grade chemical hydrometallurgical oxidation of micro-disseminated gold ores.

Experimental

Sample preparation

Pyrite samples collected from an active mine contained few impurities and exhibited a high degree of crystallization. High-grade ore was selected by hand and coarsely crushed to < 2 mm. The sample was then sorted on shaking tables and the concentrate was dried at low temperatures. The sample was further pulverized and split into five size fractions: < 0.038 mm, 0.045–0.038 mm, 0.075–0.045 mm, 0.120–0.075 mm, and 0.180–0.120 mm, and sealed in jars. The theoretical mass fractions of sulphur and iron in stoichiometric pyrite (FeS_2) are 46.55% and 53.45%, respectively. For the pyrite sample used in this study, the sulphur and iron contents are 42.18% and 50.26%, respectively, and sample purity was determined to be 92.44% (Figure 1).

Experimental methods

The leaching experiments were performed on a magnetic stirrer. Leaching agent at a predetermined concentration was added to the beaker and stirring was initiated. A predetermined amount of pyrite was added when the temperature of the leaching agent reached target. Following addition of the pyrite, a 3 mL sample of the solution was taken every 30 minutes for the first 2 hours, and every hour for each subsequent hour of the experiment. To stop further reaction within the sample, samples were immediately filtered and diluted following collection. To keep the total volume of the solution unchanged, 3 mL of fresh leaching agent of the same concentration as the initial reagent was added to the beaker after each sample was taken. The leaching progress is indicated by the leaching rate of iron from the pyrite. The concentration of iron ions in the solution was analysed using a UV-visible spectrophotometer. Following completion of the leaching experiment, the leach residue was filtered, dried at low temperature, and then saved for examination by scanning electron microscopy (SEM).

Results and discussion

Effects of $K_2S_2O_8$ concentrations on pyrite leaching

Figure 2 displays the effect of $K_2S_2O_8$ concentration on pyrite leaching at a pyrite concentration of 10 g/L, temperature of 70°C, stirring rate of 500 r/min, and a pyrite particle size of 0.075–0.045 mm.

From the data presented in Figure 2, it can be concluded that at $K_2S_2O_8$ concentrations between 0.111 mol/L and 0.555 mol/L, the leaching rate of iron from pyrite first increase with increasing $K_2S_2O_8$ concentration, then decrease, and then increases again. At $K_2S_2O_8$ concentrations less than 0.407 mol/L, the leaching rate and speed of the reaction both increase with increasing $K_2S_2O_8$ concentration. This is because there is less sulphate radical anion (SO_4^-) in the low-concentration reagent, and the probability of reaction between pyrite and peroxydisulphate can be improved by increasing the concentration of the solution. At $K_2S_2O_8$ concentrations between 0.407 and 0.418 mol/L, the leaching rate of iron from pyrite decreases with increasing $K_2S_2O_8$ concentration according to Equation [1].

$$\cdot SO_4^- + S_2O_8^{2-} \rightarrow SO_4^{2-} + \cdot S_2O_8^- \quad [1]$$

Based on this equation, it is expected that excess peroxydisulphate would function as a quenching agent to the SO_4^-, and the $S_2O_8^{2-}$ generated in Equation [1] is less utilized than SO_4^-, which has the effect of decreasing the pyrite leaching rate (Xu and Li, 2010). When the concentration of $K_2S_2O_8$ is more than 0.481 mol/L, the leaching rate of pyrite increases again with increasing $K_2S_2O_8$ concentration, presumably because the total concentration of SO_4^- and $S_2O_8^{2-}$ increases and the total oxidative capacity of the solution is greater. Based on the relationship between $K_2S_2O_8$ concentration and leaching rate and the desire to maximize the leaching rate while minimizing reagent consumption, the $K_2S_2O_8$ concentration was set at 0.407 mol/L for the following experiments.

Effects of temperature on pyrite leaching

Figure 3 displays the effect of leaching temperature on pyrite leaching at a pyrite concentration of 10 g/L, $K_2S_2O_8$ concentration of 0.407 mol/L, a stirring rate of 500 r/min, and a pyrite particle size of 0.075–0.045 mm.

It can be seen that the temperature has a significant effect on the pyrite leaching rate. The leaching rate and speed of the reaction both increase as a function of temperature. At 7 hours,

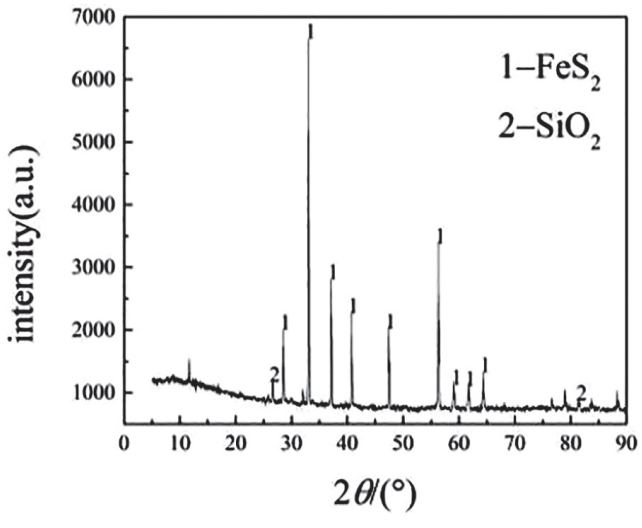

Figure 1—XRD spectrum of the pyrite sample

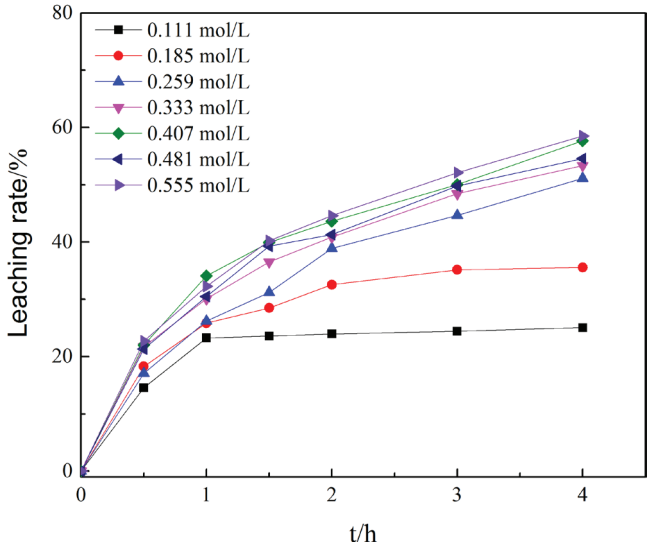

Figure 2—Effect of $K_2S_2O_8$ concentration on pyrite leaching

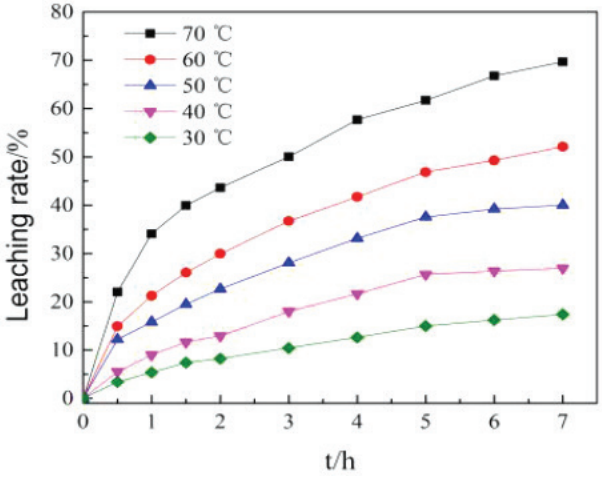

Figure 3—Effect of temperature on pyrite leaching

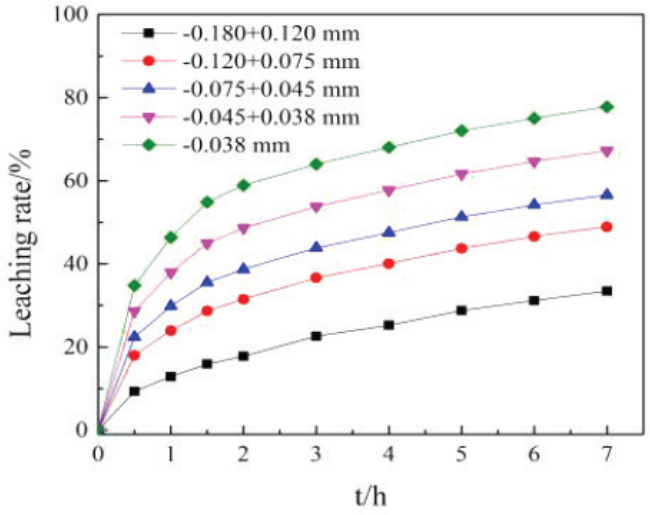

Figure 4—Effect of particle size on pyrite leaching

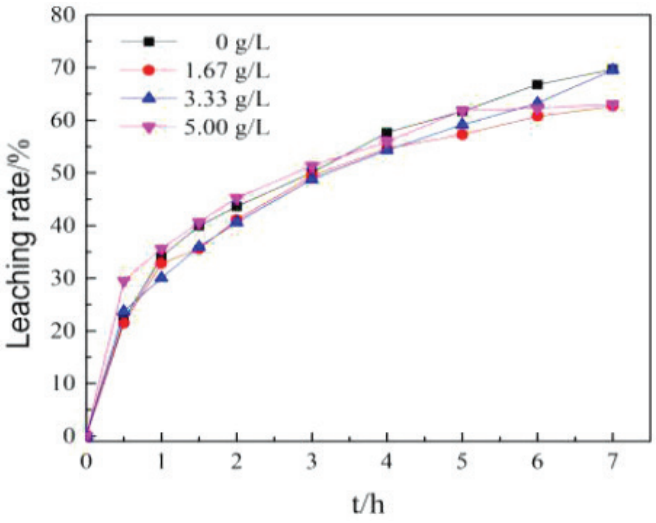

Figure 5—Effect of the ferrous sulphate concentration on pyrite leaching

the leaching rate is 17.42%; at 30°C and 65.61%. at 70°C. The relationship between leaching rate and temperature over the course of 7 hours can be expressed using the regression equation $Y = 15.38\ (e^{0.024T} - 1)$, $R_2 = 0.9980$. Thus, the leaching rate improves exponentially with temperature. This is because as the temperature increases, effective collisions between molecules during the oxidation reaction increase, and the dissolution rate of pyrite likewise increases. Based on the relationship between leaching rate and temperature and the desire to maximize reaction rates and the speed of the reaction, the temperature of the following experiments was set to 70°C.

Effects of particle size on pyrite leaching

Figure 4 displays the effect of particle size on pyrite leaching at a pyrite concentration of 10 g/L, $K_2S_2O_8$ concentration of 0.407 mol/L, stirring rate of 500 r/min, and a leaching temperature of 70°C.

It can be seen that, for a given period of time, the leaching rate and reaction speed increase with decreasing pyrite particle size. After leaching for 7 hours, the leaching rate was 33.46% for a particle size of 0.180–0.120 mm, and 80.02% for a particle size of < 0.038 mm, a relative difference of 46.56%. The reason is that the specific surface area of a particle is inversely proportional to its size (Cho *et al.*, 2017). With smaller particle sizes and a larger specific area, more FeS_2 is exposed to the $-SO_4^-$ in the solution, which improves the pyrite leaching rate. Based on the relationship between leaching rate and particle size and the desire to maximize reaction rates, the particle size was set to 0.075–0.045 mm for the following experiments.

Effects of ferrous sulphate concentration on pyrite leaching at 70°C

Figure 5 shows the effects of the ferrous sulphate concentration on pyrite leaching at 70°C, with a pyrite concentration of 10 g/L, $K_2S_2O_8$ concentration of 0.407 mol/L, stirring rate of 500 r/min, and a pyrite particle size of 0.075–0.045 mm.

From the data in Figure 5, it can be concluded that in the high-grade $K_2S_2O_8$ oxidation solution at 70°C, the ferrous sulphate concentration has a relatively minor effect on the pyrite leaching rate. There are two activation mechanisms to convert $K_2S_2O_8$ to $-SO_4^-$ – thermal activation and chemical activation (Li *et al.*, 2014). Thermal activation is the predominant mechanism at 70°C, hence the concentration of ferrous ion has little effect on the generation of $-SO_4^-$. Therefore, at 70°C, the ferrous sulphate concentration has little effect on the leaching of pyrite.

Effects of ferrous sulphate concentration on pyrite leaching at normal temperature (30°C)

Figure 6 displays the effect of the ferrous sulphate concentration on pyrite leaching at the normal leaching temperature of 30°C, a pyrite concentration of 10 g/L, $K_2S_2O_8$ concentration of 0.407 mol/L, a stirring rate of 500 r/min, and a pyrite particle size of 0.075–0.045 mm.

From the data in Figure 6, it can be concluded that when the ferrous sulphate concentration is zero, the leaching ratio of iron from pyrite increases slowly over time, achieving a rate of 16.59% over 12 hours. The leaching rate and reaction speed can be effectively improved by increasing the concentration of ferrous sulphate. This is because the Fe^{2+} in ferrous sulphate can catalyse the generation of $-SO_4^-$ from peroxysulphate. As the concentration of ferrous sulphate is increased from 1.67 g/L to 5.00 g/L, the leaching rate of pyrite is improved. However, further increases in ferrous sulphate concentration have little effect on the leaching rate. This suggests that a low concentration of Fe^{2+} is sufficient to catalyse the generation of $-SO_4^-$ from $K_2S_2O_8$.

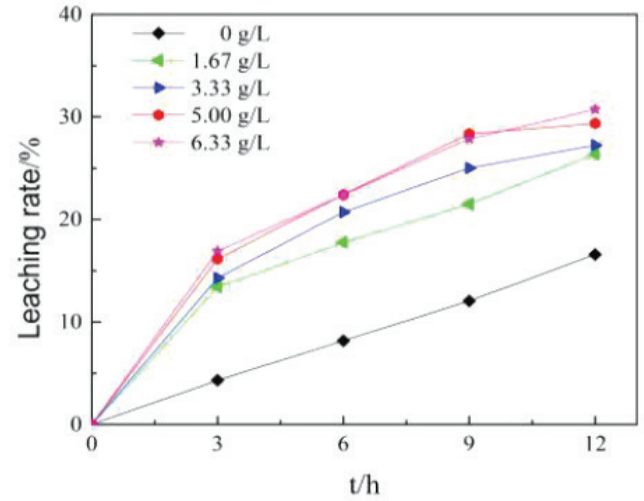

Figure 6—Effect of ferrous sulphate concentrations on pyrite leaching at 30°C

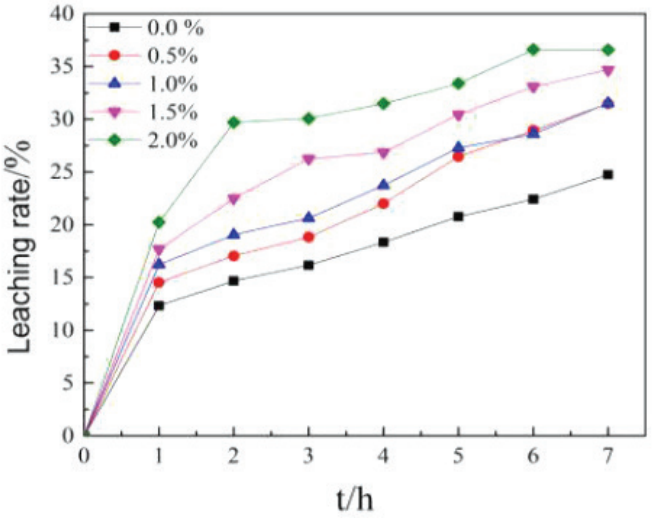

Figure 7—Effect of volumetric H_2O_2 concentration on pyrite leaching at 30°C

Effects of volumetric H_2O_2 concentration on pyrite leaching at normal leaching temperatures

Figure 7 displays the effect of volumetric concentration of H_2O_2 on pyrite leaching at 30°C at a pyrite concentration of 10 g/L, a $K_2S_2O_8$ concentration of 0.407 mol/L, a ferrous sulphate concentration of 5.00 g/L, a stirring rate of 500 r/min, and a pyrite particle size of 0.075–0.045 mm.

Increasing the H_2O_2 concentration can increase the leaching rate of iron from pyrite, and both the pyrite leaching rate and the speed of iron release are proportional to the H_2O_2 concentration. At 7 hours, the leaching rate at an H_2O_2 concentration of 2% was 36.60%, which is 11.85% higher than the leaching rate of 24.75% with no H_2O_2 added. During the initial stage of the experiment, bubbles generated in the solution were observed, and the formation of bubbles increased with increasing H_2O_2 concentration. The reason is that hydrogen peroxide can quickly generate hydroxyl radicals (OH^-) through the catalysis of Fe^{2+}, and the combined effect of $-OH^-$ and $-SO_4^-$ can increase the speed of the leaching reaction. Additionally, the total oxidation capacity is enhanced by the input of H_2O_2 (Fischbacher, von Sonntag, and Schmidt, 2017), thus improving the leaching rate of iron from pyrite.

Kinetics of oxidative pyrite leaching

Pyrite leaching is a fluid-solid two-phase reaction, and the leaching rate might be controlled by liquid film diffusion, solid film diffusion (the slowest process in surface oxidation), or a combination of these mechanisms (Zhong *et al.*, 2013). Assuming that the pyrite particles in the fluid-solid two-phase reaction may be approximated as spheres of the same size, that the concentration of the leaching agent is maintained constant, and that the leaching process is controlled by chemical reaction, the kinetic equation of a shrinking core model can be expressed as:

$$kt = 1-(1-x)^{1/3} \quad [2]$$

Liu (2012) and Zhong *et al.* (2013) used Equation [2] to investigate the oxidation kinetics of pyrite in sulphuric acid media, and concluded that the apparent activation energy of pyrite leaching is 37 kJ/mol with a Fe^{3+} concentration of 30 g/L and at temperatures between 45°C and 90°C. When the concentration of the leaching agent is altered during the course of the reaction, leaching is controlled by solid film diffusion in the remaining solid, and the kinetic equation for the shrinking core model can be expressed as:

$$kt = 1-2/3x-(1-x)^{2/3} \quad [3]$$

Bingöl, Canbazoğlu, and Aydoğan (2005) proposed a kinetic model based on the interface mass transfer and solid film diffusion, which can be expressed as:

$$kt = \ln(1-x)^{1/3}-1+(1-x)^{-1/3} \quad [4]$$

Ekmekyapar (2003) proposed a kinetic equation controlled by combined dynamics:

$$kt = 1-2(1-x)^{1/3}+(1-x)^{2/3} \quad [5]$$

According to Equation [2], if the leaching process is controlled by chemical reaction, the linear relationship $1-(1-x)^{1/3}$ *vs.* t can be plotted as in Figure 8a. Similarly, Equations [3], [4], and [5] can be used to approximate the leaching process of pyrite, as displayed in Figure 8b, 8c, and 8d. Table I lists the correlation coefficients (R^2) of the four models, which can be used to indicate the applicability of these models.

From the results presented in Table I, it can be determined that the R^2 of the dynamics model controlled by single solid film diffusion is closest to unity, suggesting that the oxidative leaching of pyrite is primarily controlled by solid film diffusion in the remaining solid.

To determine effects of additional variables, including $K_2S_2O_8$ concentration and particle size at 70°C and $FeSO_4$ and H_2O_2 concentrations at 30°C on the pyrite leaching rate, a semi-empirical model (Equation [6]) is applied to model the effects of $K_2S_2O_8$ concentration and particle size at 70°C. An additional semi-empirical model (Equation [7]) is applied to calculate the effects of $FeSO_4$ and H_2O_2 concentrations at 30°C.

$$1-2x/3-(1-x)^{2/3} = k_0 \times c_{K_2S_2O_8}^{a} \times (d_p)^{b} \times e^{-\frac{E_a}{RT}} \times t \quad [6]$$

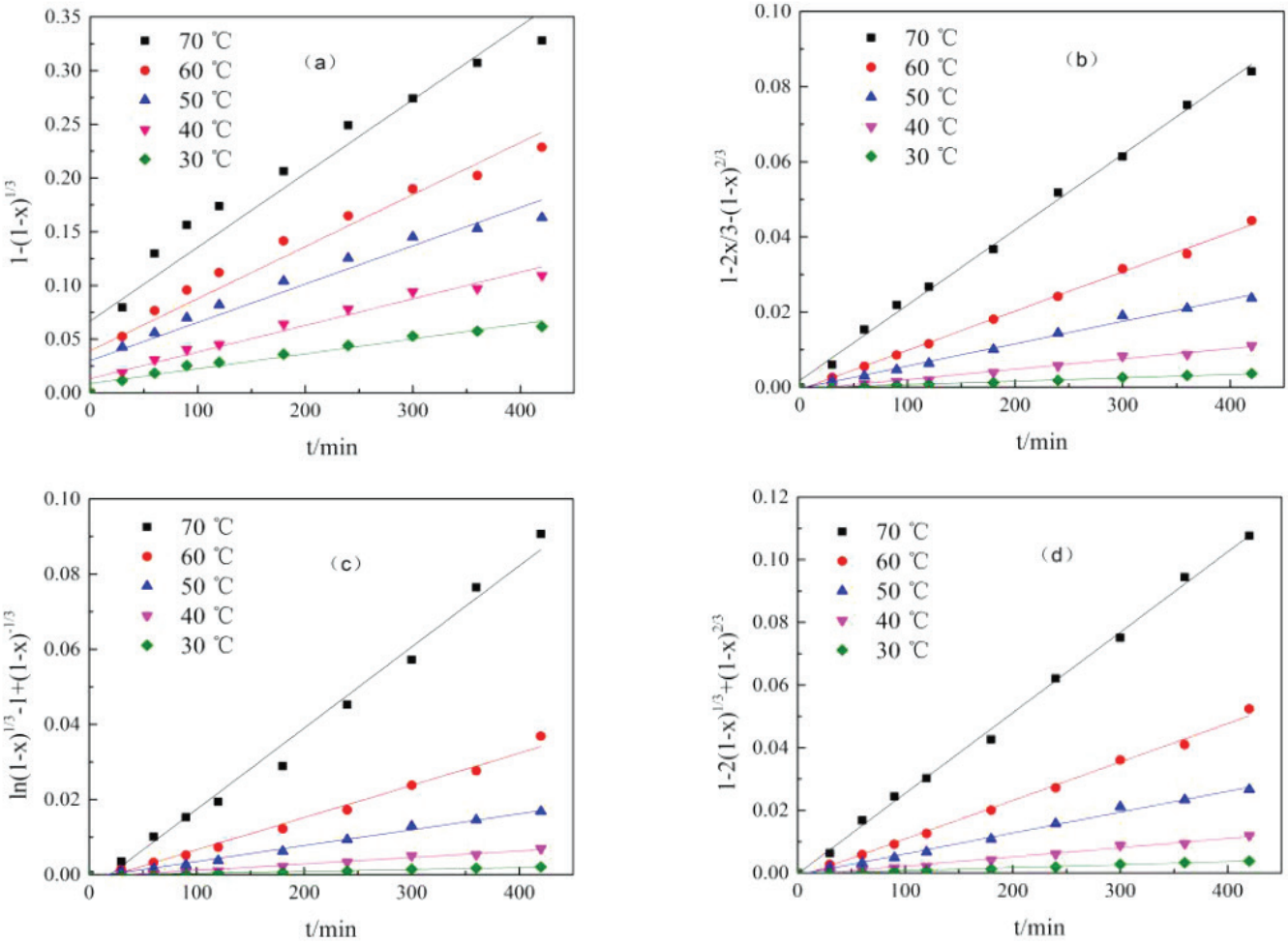

Figure 8—Kinetic model curves at four different temperatures (a) 1 – (1-x)$^{1/3}$~*t*; (b) 1-2x/3 – (1-x)$^{2/3}$~*t*; (c) 1/3ln(1 – x) – 1 + (1 – 4-x)-$^{1/3}$~*t*; (d) 1 – 2(1 – x)$^{1/3}$ + (1 – x)$^{2/3}$~*t*

Table I

Correlation coefficients (R^2) of the four dynamics models at different temperatures

T(°C)	(R^2)			
	1–(1 – x)$^{1/3}$	1–2x/3–(1-x)$^{2/3}$	ln(1 – x)$^{1/3}$-1 + (1 – x)$^{-1/3}$	1–2(1–x)1/3 + (1–x)$^{2/3}$
30	0.9558	0.9960	0.9880	0.9901
40	0.9607	0.9855	0.9797	0.9838
50	0.9284	0.9931	0.9911	0.9930
60	0.9368	0.9973	0.9849	0.9949
70	0.9105	0.9965	0.9872	0.9976

$$1-2x/3-(1-x)^{2/3} = k_1 \times c_{K_2S_2O_8}^{a} \times (d_p)^{b} \times c_{FeSO_4}^{c} \times c_{H_2O_2}^{d} \times e^{-\frac{E_a}{RT}} \times t \quad [7]$$

where x is the leaching rate; k_0, k_1 are the constants representing the reaction rate, $c_{K_2S_2O_8}$ is the concentration of $K_2S_2O_8$ in mol/L; c_{FeSO_4} is the concentration of $FeSO_4$ in mol/L; $c_{H_2O_2}$ is the concentration of H_2O_2 in mol/L; d_p is the particle size in mm; t is the reaction time in minutes; and T is the temperature in kelvin.

If the concentration of $K_2S_2O_8$ is modified while other conditions are kept the same, Equation [6] can be expressed as:

$$\cdot 2x/3-(1-x)^{2/3} = k_2 \times c_{K_2S_2O_8}^{a} \times t \quad [8]$$

$$\frac{d\left[1-2x/3-(1-x)^{2/3}\right]}{dt} = k_2 \times c_{K_2S_2O_8}^{a} \quad [9]$$

Figure 9 displays curves representing the relationships between $K_2S_2O_8$ concentration and time according to Equation [9]. The slopes represent the values of d[1 – 2x/3 – (1 – x)$^{2/3}$]/*dt* corresponding to different $K_2S_2O_8$ concentrations. Similarly, Figures 9b and 9c display curves representing the relationships

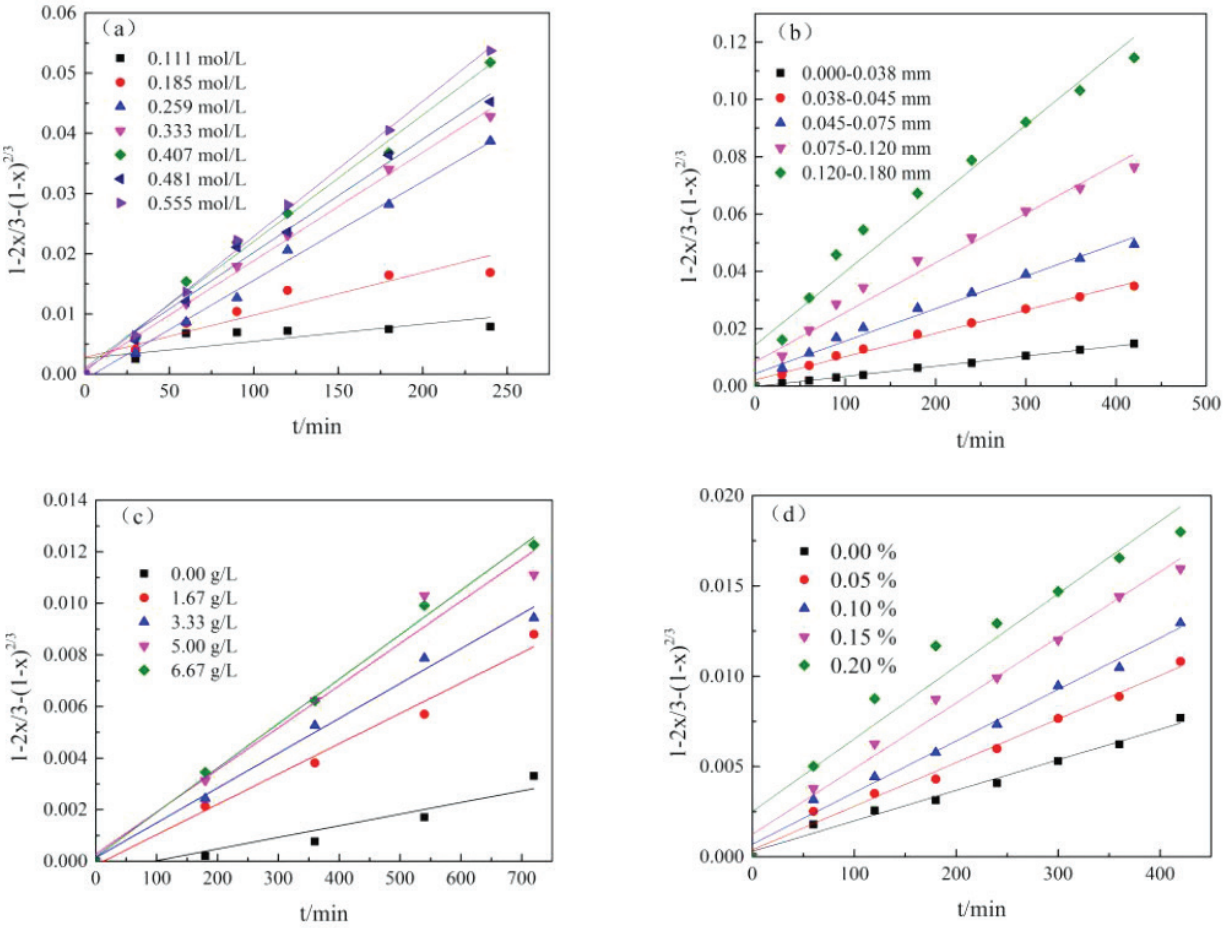

Figure 9—Plots of 1 – 2x/3 – (1– x)$^{2/3}$ *vs. t* as a function of: (a) $K_2S_2O_8$ concentration; (b) particle size ; (c) $FeSO_4$ concentration; (d) H_2O_2 concentration

between $K_2S_2O_8$ concentrations and time at different particle sizes, $FeSO_4$ concentrations, and H_2O_2 concentrations. The slope of $\ln[d[1 - 2x/3 - (1 - x)^{2/3}]/dt]$ *vs* $\ln c_{K_2S_2O_8}$ is 0.431 as shown in Figure 9a; that of $\ln[d[1 - 2x/3 - (1 - x)^{2/3}]/dt]$ *vs* ln*dp* is –0.920; that of $\ln[d[1 - 2x/3 - (1 - x)^{2/3}]/dt]$ *vs* $\ln c_{FeSO_4}$ is –0.295; and that of $\ln[d[1 - 2x/3 - (1 - x)^{2/3}]/dt]$ *vs* $\ln c_{H_2O_2}$ is 0.378, as shown in Figure 10.

If the temperature is changed but other conditions remain constant, the slopes of the lines in Figure 8 represent the reaction rate constants at different temperatures, which can be expressed as Equation [10].

$$k = A \cdot e^{-\frac{E_a}{RT}} \qquad [10]$$

where k is the reaction rate constant; A is the frequency factor, a constant; E_a is the apparent activation energy; R is the ideal gas constant; and T is the temperature in kelvin.

Taking the logarithm on both sides of Equation [10] yields Equation [11]:

$$\ln k = \ln A - \frac{E_a}{RT} \qquad [11]$$

Figure 11 shows the Arrhenius curve for oxidative pyrite leaching, where $1/T$ is plotted on the x-axis and lnk on the y-axis. From the approximate slope of the curve, the apparent activation energy of pyrite leaching over the temperature range 30–70°C is 65.30 kJ/mol, within the previously reported range of 46–98 kJ/mol (Zhong, 2015).

By inputting the values for *a, b, c, d,* and E_a into Equations [6] and [7], the statistical average values of k_0 and k_1 are shown to be $k_0 = 2.3 \times 10^5$ min^{-1}, $k_1 = 5.2 \times 10^5$ min^{-1}. The resulting kinetic equation for oxidative pyrite leaching at 70°C is:

$$1 - 2x/3 - (1-x)^{2/3} = 2.35 \times 10^5 \times c_{K_2S_2O_8}^{0.431} \times (d_p)^{-0.920} \times e^{-\frac{7853.5}{T}} \times t \qquad [12]$$

When ferrous sulphate and hydrogen peroxide are added to the potassium peroxydisulphate single system at the normal leaching temperature of 30°C, the kinetic equation for the leaching reaction that expresses the effects of their concentrations is:

$$1 - 2x/3 - (1-x)^{2/3} = 2.28 \times 10^5 \times c_{K_2S_2O_8}^{0.431} \times (d_p)^{-0.920} \times c_{FeSO_4}^{0.295} \times c_{H_2O_2}^{0.378} \times e^{-\frac{7853.5}{T}} \times t \qquad [13]$$

Scanning electron microscopy

SEM images of pyrite before and after oxidative leaching are shown in Figure 12.

Prior to leaching, pyrite samples exhibited a compact structure and regular morphology with no fracture or pores. Pyrite samples examined after 3 hours of leaching exhibited some

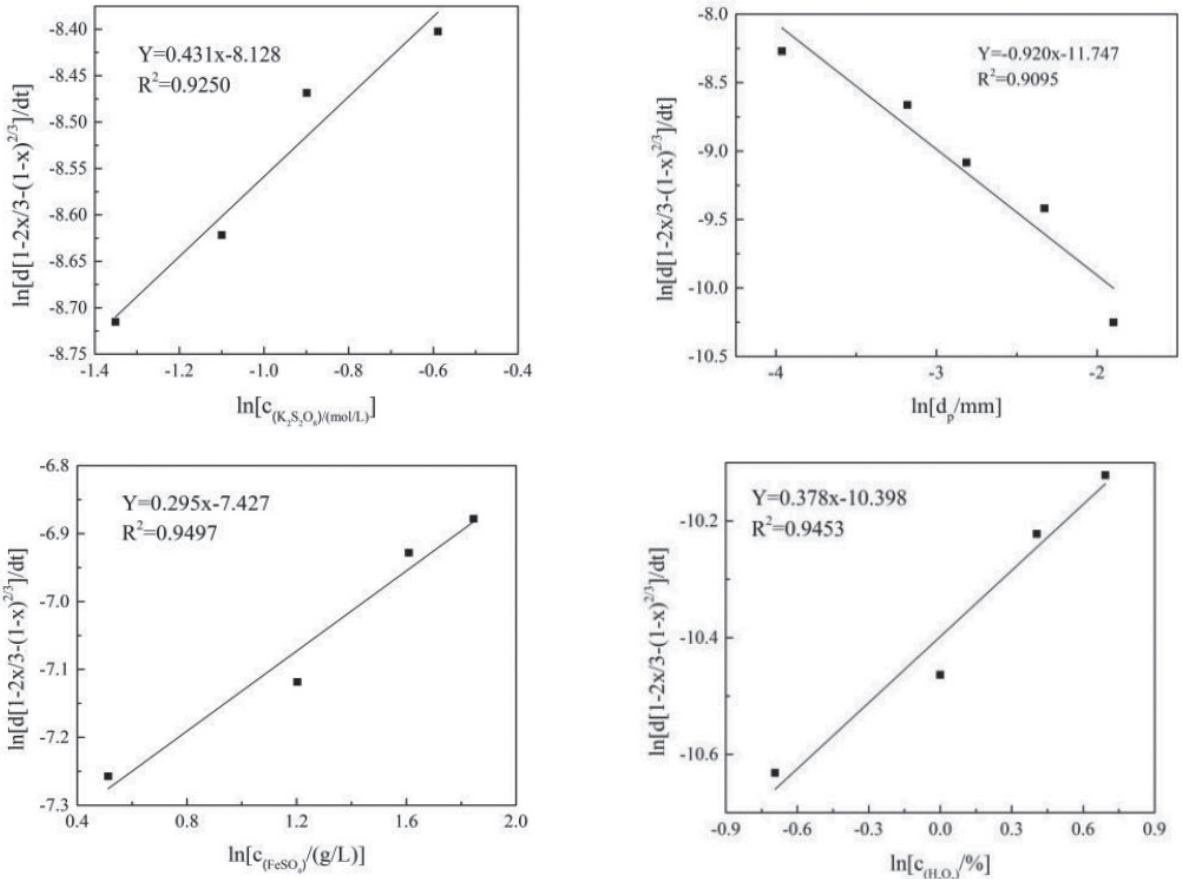

Figure 10—Plots of $\ln[d[1-2x/3-(1-x)^{2/3}]/dt]$ **and** $\ln[c_{(K_2S_2O_8)/(\mathrm{mol/L})}]$, $\ln[d_p/\mathrm{mm}]$, $\ln[c_{(\mathrm{FeSO_4})/(g/L)}]$, $\ln[c_{(H_2O_2)/\%}]$

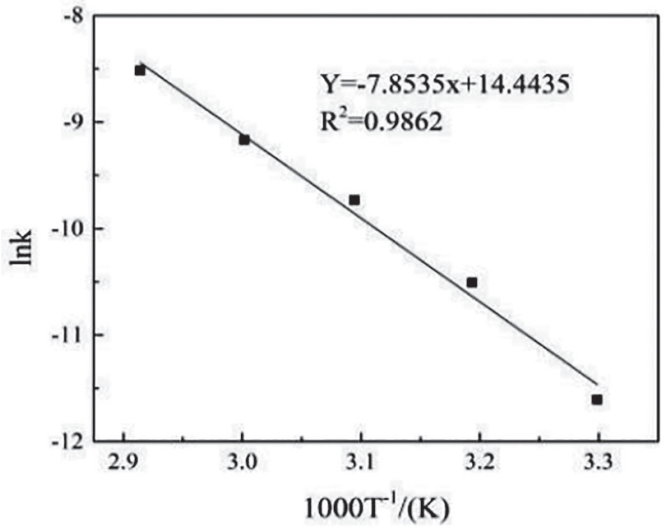

Figure 11—Arrhenius curve for oxidative pyrite leaching

cracks and hollows. After leaching for 7 hours, pyrite exhibited severely eroded surfaces and many faviform holes.

Conclusion

This study investigated the impacts of potassium persulphate concentration, leaching temperature, pyrite particle size, and the presence of ferrous sulphate and hydrogen peroxide on pyrite leaching using potassium persulphate as the oxidizing agent in a single system of potassium persulphate and a combined system of potassium persulphate plus ferrous sulphate. The following conclusions are derived.

- At a $K_2S_2O_8$ concentration of 0.111–0.555 mol/L, the leaching rate of iron from pyrite first increases with increasing $K_2S_2O_8$ concentration, and then falls. The leaching rate reaches a peak value of 73.69% at a $K_2S_2O_8$ concentration of 0.407 mol/L. The leaching rate is also positively correlated with temperature, as it increases by 48.19% when the temperature is raised from 30°C to 70°C. An exponential relationship can be derived between the leaching rate and temperature, which can be approximated by the formula: $Y = 15.38(e^{0.024T} - 1)$, $R^2 = 0.9980$.
- The leaching rate and speed are both inversely proportional to the pyrite particle size. After leaching for 7 hours, the leaching rate of the sample with particle size 0.180–0.120 mm reaches to 33.46%, and that of the sample with particle size < 0.038 mm is 80.02%. The difference between these two values is 46.56%. Adding ferrous sulphate and hydrogen peroxide at the normal leaching temperature of 30°C can also enhance the leaching of pyrite. However, the ferrous sulphate concentration has no impact on the pyrite leaching reaction.
- Pyrite leaching follows the kinetic equation $1 - 2/3x - (1 - x)^{2/3} = kt$, which is controlled by solid film diffusion in the remaining solid. A kinetic equation for oxidative pyrite

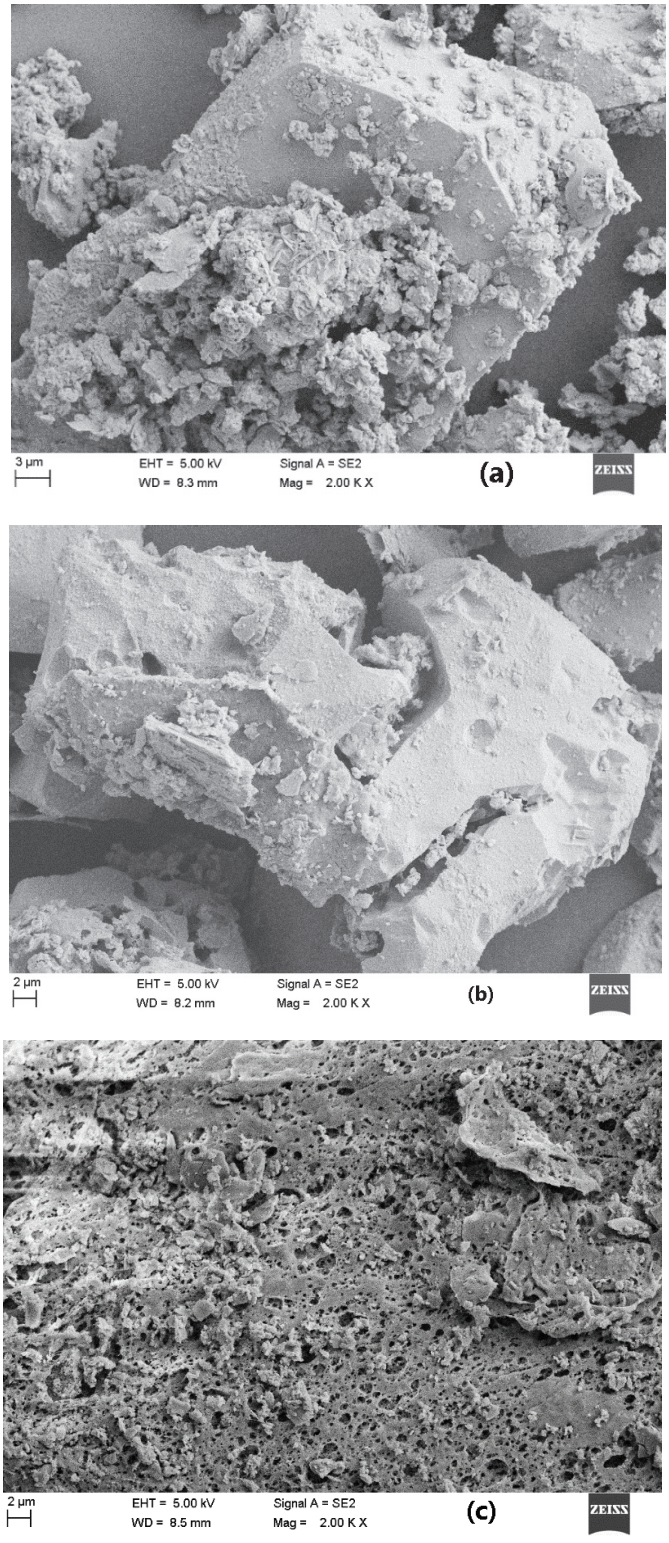

Figure 12—SEM images of pyrite (a) before leaching, (b) after leaching 3 hours, and (c) after leaching for 7 hours

leaching at 70×C is derived by approximating the leaching processes as two different systems:

$$1-2x/3-(1-x)^{2/3} = 2.35\times10^{5}\times c_{M_2S_2O_8}^{0.431}\times\left(d_p\right)^{-0.920}\times e^{-\frac{7853.5}{T}}\times t$$

The kinetic equation for leaching that considers concentrations of ferrous sulphate and hydrogen peroxide at normal temperatures of 30°C is:

$$1-2x/3-(1-x)^{2/3} = 2.28\times10^{5}\times c_{M_2S_2O_8}^{0.431}\times\left(d_p\right)^{-0.920}\times c_{FeSO_4}^{0.295}\times c_{H_2O_2}^{0.378}\times e^{-\frac{7853.5}{T}}\times t$$

Pyrite samples exhibit a regular morphology before leaching, but faviform holes on the surface after leaching.

Acknowledgements

This work was supported by National Natural Science Foundation of China (51864010), the Plan Project of Science and Technology of Guizhou Province of China (Qiankehe Foundation [2017]1404 and Qiankehe Platform Talents [2018]5781) and the Postgraduate Scientific Research Foundation of Guizhou Province of China (Qianjiaohe YJSCXJH (2018)082). We thank Dr Guy Evans from Liwen Bianji, Edanz, Editing China (www.liwenbianji.cn/ac), for editing the English text of a draft of this manuscript.

References

Bingol, D., Canbazoglu, M., and Aydogan, S. 2005. Dissolution kinetics of malachite in ammonia/ammonium carbonate leaching. *Hydrometallurgy*, vol. 76, no. 1-2. pp. 55–62.

Cho, T.Y., Yoon, J.H., Yoon, S.H., Joo, Y.K., Choi, W.H., and Son, Y.B. 2017. The effects of particle size on the surface properties of an HVOF coating of WC-Co. *Korean. Journal of Metals and Materials*, vol. 55, no. 4. pp. 227–231.

Ekmekyapar, A.O.R.K.A. 2003. Dissolution kinetics of an oxidized copper ore in ammonium chloride solution. *Chemical and Biochemical Engineering Quarterly*, vol. 4, no. 17. pp. 261–266.

Fischbacher, A., Von Sonntag, C., and Schmidt, T.C. 2017. Hydroxyl radical yields in the Fenton process under various pH, ligand concentrations and hydrogen peroxide/Fe(II) ratios. *Chemosphere*, vol. 182. pp. 738–744.

Gozmen, B., Kayan, B., Gizir, A.M., and Hesenov, A. 2009. Oxidative degradations of reactive blue 4 dye by different advanced oxidation methods. *Journal of Hazardous Materials*, vol. 168, no. 1. pp. 129–136.

Gu, G.H., Su, L.J., Chen, M.I., Sun, X.J., and Zhou, H.B. 2010. Bio-leaching effects of Leptospirillum ferriphilum on the surface chemical properties of pyrite. *Mining Science and Technology*, vol. 20, no. 2. pp. 286–291 [In Chinese].

Hillesa, A.H., Abu Amrb, S.S., Husseina, R.A., El-Sebaiea, O.D., and Arafa, A.I. 2016. Performance of combined sodium persulfate/H_2O_2 based advanced oxidation process in stabilized landfill leachate treatment. *Journal of Environmental Management,* vol. 166. pp. 493–498.

Hu, J., Huang, H., Xie, H., Gan, L., Liu, J., and Long, M. 2017. A scaled-up continuous process for biooxidation as pre-treatment of refractory pyrite-arsenopyrite gold-bearing concentrates. *Biochemical Engineering Journal*, vol. 128. pp. 228–234.

Liu, Z.X. 2012. Leaching kinetics of copper bearing minerals and leaching process of copper oxide / zinc ore in ammonia solution. PhD thesis, Central South University, China.[In Chinese].

Li, H.X., Wan, J.Q., Ma, Y.W., Huang, M.Z., Wang, Y., and Chen, Y.M. 2014. New insights into the role of zero-valent iron surface oxidation layers in persulfate oxidation of dibutyl phthalate solutions. *Chemical Engineering Journal*, vol. 250, no. 250. pp. 137–147.

Tang, L.J., Tang, Y., Wang, Y.N., and Yang D.Q. 2015. Study on alkaline pretreatment and non cyanide leaching of fine disseminated gold ore. *Gold Science and Technology*, vol. 23, no. 5. pp. 94–98 [In Chinese].

Xu, X.R. and Li, X.Z. 2010. Degradation of azo dye Orange G in aqueous solutions by persulfate with ferrous ion. *Separation and Purification Technology*, vol. 72, no. 1. pp. 105–111.

Zhong, L., Wu, Z., Huang, Z., and Guo, Z. 2013. Oxidation kinetics of gold bearing pyrite in sulfuric acid medium. *Rare Metals*, vol. 37, no. 2. pp. 295–301.

Zhong, S.P. 2015. Leaching kinetics of gold bearing pyrite in H_2SO_4–$Fe_2(SO4)_3$ system. *Transactions of Nonferrous Metals Society of China*, vol. 25, no. 10. pp. 3461–3466.

Zhao, H., Wang, J., Gan, X., Hu, M., Tao, L., Qin, W., and Qiu, G. 2016. Role of pyrite in sulfuric acid leaching of chalcopyrite: An elimination of polysulfide by controlling redox potential, *Hydrometallurgy*, vol. 164. pp. 159–165. ◆